The genetic architecture of host response suggests a trade-off between mycorrhizal and non-mycorrhizal performance in field-grown maize

M. Rosario Ramírez-Flores[1], Sergio Perez-Limón[2], Meng Li[3], Benjamin Barrales-Gamez[2], Víctor Olalde-Portugal[1] and Ruairidh J. H. Sawers[3*]

[1] Departamento de Biotecnología y Bioquímica, Centro de Investigación y de Estudios Avanzados (CINVESTAV-IPN), Irapuato, C.P. 36821, Guanajuato, México.

[2] Laboratorio Nacional de Genómica para la Biodiversidad/Unidad de Genómica Avanzada, Centro de Investigación y de Estudios Avanzados, Instituto Politécnico Nacional (CINVESTAV-IPN), Irapuato, C.P. 36821, Guanajuato, México

[3] Department of Plant Science, The Pennsylvania State University, State College, PA, USA.

* Author for correspondence: rjs6686@psu.edu

Main text word count: 4673

Number of Figures: 5

Number of Tables: 1

Abstract

Arbuscular mycorrhizal fungi (AMF) are ubiquitous in cultivated soils, forming symbiotic relationships with the roots of major crop species. Although physiological and molecular genetic studies have demonstrated the potential of the symbiosis to enhance host plant nutrition and alleviate environmental stress, experimental difficulties have complicated estimation of the actual benefit in the field. Furthermore, host response to the symbiosis can range from positive to negative depending on the plant variety. Here, a novel mapping strategy, based on the use of AMF-resistant plant varieties, was implemented to evaluate maize response to arbuscular mycorrhiza in the field. AMF were found to make a significant contribution to plant growth and yield components, both in terms of absolute affect and as a driver of variation among plant genotypes. Characterization of the genetic architecture of host response distinguished mycorrhiza dependence and benefit and indicated genetic trade-off between mycorrhizal and non-mycorrhizal growth. This approach is applicable to other crop species, permits further mechanistic analysis and is scalable to yield trials.

Introduction

There is a pressing need to develop sustainable agricultural systems that improve productivity while minimizing adverse environmental impacts (Foley et al. 2011; Lynch, 2019). In the face of this challenge, there is great interest in the potential benefits of arbuscular mycorrhizal (AM) symbiosis and other microbial mutualisms to enhance crop production (e.g. Sawers *et al.*, 2008; Fester & Sawers, 2011; Bender et al., 2016). Indeed, many commercial "biofertilizers" are already on the market (Faye *et al.*, 2013). Nonetheless, the value of the AM symbiosis to agriculture remains a matter of debate (Ryan and Graham 2018; Rillig et al. 2019). Experimental studies under controlled conditions suggest that AMF have much to offer host plants, including enhanced uptake of immobile soil nutrients - especially phosphorus (P) - and water, and improved tolerance to a range of abiotic and biotic stresses (Borowicz 2001; Chandrasekaran et al. 2014; Augé et al. 2014; Chiu & Paszkowski, 2019). AMF also contribute important ecosystem services (van der Heijden et al. 2015), including promoting soil aggregation (Rillig and Mummey 2006), and reducing nutrient loss through leaching and emission (Bender et al. 2014; Cavagnaro et al. 2015). Yet efforts to integrate AMF into modern agriculture, whether by targeted management of the AMF community or breeding more AM compatible crops (Fester & Sawers, 2011; Bender et al. 2016), are hampered by the difficulties of evaluating host response in the field where both crop choices and soil management practices affect AMF communities, and appropriate AMF free controls are hard to obtain.

While AM symbiosis dates back over 450 million years (Strullu-Derrien *et al.*, 2018), agriculture is a recent development - our major crops being domesticated within the last ~10,000 years, and modern varieties being the product of the last ~50 years of intensive selection. Modern breeding efforts have focused on maximizing yield under homogeneous environments

with large quantities of synthetic inputs. It is not clear how the breeding process has impacted the balance of AM symbiosis (discussed in Sawers *et al.*, 2008, 2018), but major crops do retain the capacity to interact with AMF and they conserve the necessary molecular machinery (*e.g.* Gutjahr et al., 2008; Nadal et al., 2017). Modern crop varieties differ in response to AM colonization (Hetrick *et al.*, 1992; Kaeppler *et al.*, 2000; Sawers *et al.*, 2010; Mascher *et al.*, 2014; Sawers *et al.*, 2017; Watts-Williams *et al.*, 2019), raising important fundamental questions, but implying that there is scope for optimization through breeding or genetic manipulation. To be successful, however, any such improvement strategy will require increased understanding of the genetic and mechanistic basis of host response.

Defining variation in host response to AMF can be challenging (discussed in Janos, 2007; Sawers *et al.*, 2010). Here, host response is defined as the difference between mycorrhizal and non-mycorrhizal plants, applied to any phenotypic measurement. In addition, *dependence* is defined as the capacity of a given variety to perform in the absence of AMF (Janos, 2007), and *benefit* as the degree to which a plant host profits from the association. Crucially, variation in host response confounds differences in both dependence and benefit. The optimization of AM symbiosis in crop varieties is concerned with benefit: there is no interest in elevating host response by increasing dependence (Sawers *et al.*, 2008).

In this study, variation in maize performance in the field was genetically mapped in both the presence and absence of AM colonization. To distinguish dependence and benefit, the concepts of genotype x environment interaction (Des Marais & Juenger, 2010) were applied to the mycorrhizal and non-mycorrhizal “environments”. Field-grown, non-colonized plants were obtained by generation of AM resistant families using knowledge of mutants previously identified in rice (Gutjahr *et al.*, 2008). The results of this study indicate that AM symbiosis

makes a substantial contribution to maize performance in the field. Estimation of performance potential at the whole genome level found evidence of a trade-off between mycorrhizal and non-mycorrhizal growth.

Materials and Methods

Plant material and generation of the $F_{2:3}$ mapping population

An $F_{2:3}$ population was developed from the cross between a W22 stock homozygous for the *hun1-2* allele (*Mutator* insertion mu::1045305 in the gene GRMZM2G099160/Zm00001d012863. www.maizegdb.org. Ramírez-Flores MR. M.Sc. thesis, 2015) and the subtropical CIMMYT inbred line CML312. The F_1 was self-pollinated to generate an F_2 segregating *hun1-2* and W22/CML312 genome content. F_2 plants were genotyped by PCR to identify homozygous wild-type and mutant individuals, and these self-pollinated to generate susceptible (*AMF-S*) and resistant (*AMF-R*) $F_{2:3}$ families, respectively. $F_{2:3}$ families were increased by sibling-mating. Material was generated in Valle de Banderas, Nayarit, Mexico and Irapuato, Guanajuato, Mexico from 2016 to 2019. Small amounts of seed are available for distribution through direct contact with the authors.

DNA extraction and PCR genotyping of hun1-2

DNA extraction was performed as described in by Fulton *et al.*, 1995. The genotype at the *Hun* locus was determined by running wild-type and mutant PCR reactions. To amplify the wild-type fragment, a pair of gene-specific primers were used (HUNF01-CGCGAAGAAACGCAGACATTCC and HUNR04-TAACCTGGAGCGAACAGAATCCAC), generating a product of 606 bp. To amplify the mutant fragment a combination of *Mutator*

primer and gene-specific primer were used (HUNF03-CTTGGGCGCATTGGAAATTCATCG and RS183-CGCCTCCATTTCGTCGAATCCSCTT), generating a fragment of 839 bp. PCR conditions were: 1 cycle of initial incubation at 94ºC for 3 min, 32 cycles of 94ºC for 30 sec, 60ºC for 30 sec and 72ºC for 1 min, and 1 cycle of a final extension at 72ºC for 5 min. PCR used the Kapa Taq PCR kit from Kapa Biosystems (Wilmington, Massachusetts, United States) following the manufacturer's instructions. Products were visualized on 1 % agarose gel.

Whole genome genotyping and genetic map construction

Approximately 200 F_2 parents were analyzed using the Illumina MaizeLD BeadChip (https://www.illumina.com/products/by-type/microarray-kits/maize-ld.html). Over 3,000 single nucleotide polymorphisms (SNPs) were detected, with a call rate of> 96% for all samples. The SNP set was processed using TASSEL 5 (Bradbury *et al.*, 2007). SNPs were transformed to ABH format (A: CML312; B: W22) and filtered to remove sites matching any of the following criteria: > 30% missing data; monomorphic sites outside of the *Hun* locus; SNPs outside the *Hun* locus showing segregation distortion ($\square^2$ test, $p < 0.05$); redundant sites. The markers "5_2269274", "5_3096229" and "5_4270584" (physical position on chromosome 5 at 2.67, 3.1 and 4.27 Mb, respectively) were used to confirm the expected genotype at the *Hun* locus. The genetic map was built in R (R core team 2020) using R/ASMAP (Taylor & Butler, 2017) and R/qtl (Broman *et al.*, 2003; Broman & Sen, 2009).

Field Evaluation and phenotypic analysis

The $F_{2:3}$ population was evaluated in the summer of 2019 at the UNISEM experimental station in Ameca, Jalisco, Mexico (20.78, -105.243). Three complete blocks of 75 *AMF-S* and 66 *AMF-R*

families were evaluated. Within each block, AMF-S an AMF-R families were alternated. The order of the families within the *AMF-S* or *AMF-R* sub-populations was randomized within each block. For each replicate, 45 seeds of each family were sown in a plot of three 2 m long rows. Only the second row of each plot was considered for evaluation, the first and third rows providing a buffer between adjacent families. Phenotypic data were collected at flowering and after harvest as follows: stand count (STD), number of plants per row; days to anthesis (DTA), number of days from planting until anthers visible on the main spike of half of the plants in the row; days to silking (DTS), number of days from planting until silks visible on half of the plants in the row; anthesis-silking interval (ASI), difference in days between anthesis and silking; plant height (PH), distance in cm from the ground to the flag leaf; tassel branch number (TBN), number of primary lateral branches originating from the main spike; ear weight (EW), the weight in g of the ear; ear length (EL), distance in centimeters from the base to the tip of the ear; ear diameter (ED), the diameter in cm at the middle part of the ear; kernel row number (KRN), number of rows in the middle part of the ear; kernels per row (KPR), number of kernels in a single row from the base to the tip of the ear; cob diameter (CD), diameter in cm at the middle part of the cob; fifty kernel weight (FKW), weight in g of 50 randomly selected kernels; total kernel weight (TKW), weight in g of all kernels on the ear; total kernel number (TKN), estimated from TKW/FKW * 50.

Image analysis

Image-based phenotyping method was used to quantify the size and shape of maize ear, cob, and kernel. Ears and cobs (1-3) from each plot, and approximately 50 kernels from associated ears, were scanned using an Epson Perfection V600 scanner at 1200 dots per inch. Scanned images

were uploaded to Cyverse (Merchant *et al.*, 2016) and analyzed using an automatic pipeline to quantify ear, cob, and kernel attributes (Miller *et al.*, 2017). Width profiles of ear and cob and contour data of kernels were extracted in R to compute their shapes.

Principal Component Analysis

Principal Component Analysis (PCA) was conducted to analyze major sources of plant phenotypic variance and to visualize the relationships among all measured phenotypic traits across two maize families. PCA was performed using the prcomp function in R.

QTL mapping and whole genome prediction

QTL mapping was performed using the R/qtl package (Broman *et al.*, 2003) on a population composed of 73 AMF-S and 64 AMF-R F2:3 families. Single-QTL standard interval mapping was run using the scanone function with Haley-Knott regression, with the genotype at *Hun* (wt =1; *Hun* = 0) treated as a covariate (hereafter, AMF). To assess QTL x AMF interaction (Broman & Sen, 2009), QTL analysis was performed under four different models: separate analyses for AMF-S (H_{0wt}) and AMF-R (H_{0hun}) subpopulations; considering AMF as an additive covariate (H_a) and considering AMF as an interactive covariate (H_f). The LOD significance threshold for each trait and model was established with a permutation test ($\alpha = 0.05$, 1000 permutations). Evidence of QTL x AMF interaction was obtained by comparing H_f and H_a models, where the difference $LOD_i = LOD_f - LOD_a$ was considered with reference to the threshold difference $LOD_thr_i = LOD_thr_f - LOD_thr_a$ for evidence of possible interaction. Individual QTL were combined into multiple-QTL models on a per trait basis. Where evidence was found of QTL x AMF interaction in the single scan, the interaction was also included in the

multiple-QTL model. Multiple-QTL models were evaluated using the fitqtl function and non-significant ($p < 0.1$) terms removed according to the drop-one table.

To compare the potential of a given genotype in the presence or absence of AM colonization, we estimated the performance of the 137 families for both levels of AMF using two approaches. In the first approach, we generated fitted values from the multiple-QTL models, under both levels of the AMF covariate. In the second approach, we performed whole genome prediction using the R/rrBLUP package (Endelman, 2011). Missing genotypes were imputed with the A.mat function and marker effects and BLUE values were obtained with the mixed.solve function. The observed values for AMF-S families were used to train a mycorrhizal model, that was then applied to the genotypes of the AMF-R families; the observed values from the AMF-R families were used to train a non-mycorrhizal model, that was then applied to the genotypes of the AMF-S families. For interpretation of the results, predicted values were compared for all genotypes in both levels of AMF, avoiding possible bias in extreme observed values.

Results

Mutation in a maize common symbiosis gene demonstrates the importance of arbuscular mycorrhizae in the field

To generate AMF-resistant maize varieties for use in field experiments, the maize gene-model set (www.maizegdb.org) was searched for sequences orthologous to the essential common-symbiosis genes *CASTOR* and *POLLUX* (*DMI1*) (Parniske, 2008). *CASTOR* and *POLLUX* were found to be single copy genes in maize, and designated *Hunahpu* (*Hun1*; GRMZM2G099160; Zm00001d012863) and *Xbalanque* (*Xba1*; GRMZM2G110897; Zm00001d042694) after the hero twins of Mayan mythology (Ramírez-Flores MR. M.Sc. thesis, 2015). A survey of publicly

available reverse-genetic resources identified a W22 inbred stock carrying insertion of a *Mutator* transposon in the first exon of *Hun1* (McCarty et al., 2005). This insertion was designated *hun1-2::mu* (hereafter, *hun1-2*). In common with the *castor* mutants of lotus and rice (Gutjahr *et al.*, 2008; Charpentier *et al.*, 2008), maize plants homozygous for the *hun1-2* allele were found to be resistant to mycorrhizal colonization in greenhouse-based, controlled inoculation experiments (Supplemental Material; Ramírez-Flores MR. M.Sc. thesis, 2015). To leverage the availability of an AMF-resistance allele for the study of host response to AMF in the field, the *hun1-2* mutant was crossed to the subtropical inbred line CML312, and advanced to generate a total of 75 *hun1-2* (resistant; *AMF-R*) and 75 wild-type (susceptible; *AMF-S*) $F_{2:3}$ families for genetic mapping (see Materials and Methods; Supplemental Material).

Prior to conducting a full experiment, a subset of families were grown to maturity in the field to evaluate mycorrhizal colonization; microscopic inspection confirmed the presence of fungal structures to be greatly reduced in *AMF-R* families, while *AMF-S* families showed significant levels of colonization (Supplemental Material). In a second preliminary trial, a subset of families were grown to maturity in a highly-managed nursery field under conditions of high nutrient availability and minimal stress (drip-fertigation; sandy soil; extensive weed and pest management). Under these conditions, there was no clearly observable impact of the *hun1* mutation on plant performance nor statistical difference in plant height or flowering time between *AMF-S* and *AMF-R* families - indicating that the *hun1* mutation does not condition a general defect in plant growth or show marked pleiotropic effects beyond the block in mycorrhizal colonization (Supplemental Material).

To estimate host response, 73 AMF-S and 64 AMF-R families were evaluated in triplicate using 3-row plots (Fig. 1A; ~1, 2000 rows of 15 individuals for a total of ~ 20, 000

plants plus additional check plots) under rain-fed, medium-input, subtropical field conditions (Ameca, Mexico. 2019). On inspection, *AMF-R* families appeared to perform worse than *AMF-S* families, exhibiting mild-chlorosis (Fig. 1B), delayed silking, and visibly poorer ears (Fig. 1C-D). Among 15 collected phenological and morphological traits and yield-components (Fig. 1E-H; Materials and Methods; Supplemental Material), 11 traits showed significant marginal differences between *AMF-S* and *AMF-R* families, equating to host response ranging from 3 to 51 % (Table 1; Supplemental Material). *AMF-R* families were reduced in stature and delayed in silking (female flowering), resulting in an extension of anthesis-silking interval (ASI; Fig 1E, F; Table 1; Supplemental Material) - a classic symptom of abiotic stress in maize. Ear size (evaluated as ear length, ear diameter and analysis of scanned ear images) was reduced in *AMF-R* families, along with ear and total kernel weight (Table 1; Supplemental Material). Individual kernels were not significantly different in weight (fifty kernel weight) or size (analysis of scanned images) between *AMF-S* and *AMF-R* families (Fig. 1G; Table 1; Supplemental Material). The total number of kernels per ear, however, was greatly reduced in *AMF-R* families (Fig. 1H; Table 1), indicative of poor seed set, a possible consequence of increased ASI.

QTL x AMF effects underlie variation in mycorrhiza response

To characterize the genetic architecture of host response, a Quantitative Trait Locus (QTL) analysis was performed using the trait estimates obtained for the 137 $F_{2:3}$ families and the genotypes of their respective F_2 parents. All families were combined in a single analysis using a model that included the *Hun* genotype as an interactive covariate. Under this model, the *Hun* additive effect (hereafter, AMF effect) estimates the marginal host response across all families, QTL additive effects capture genetic differences between the parents with regard to the trait

under consideration, and QTL x AMF effects indicate underlying heritable differences in the response of the CML312 and W22 parents to mycorrhiza.

A total of 21 significant ($\alpha = 0.05$) QTLs were identified associated with traits that differed between *AMF-S* and *AMF-R* families, 17 of which also showed AMF x QTL interaction (Table 1). A further 3 QTLs were associated with non-responsive traits (GC, KRN, KC); as would be expected, the AMF term was not significant in these cases. Significant QTL, AMF and AMF x QTL terms, were combined into a single multiple-QTL model for each trait. To avoid unwarranted complexity, QTL x QTL interactions were not considered. For each trait, the percentage of phenotypic variation explained by AMF, by additive QTL and by AMF x QTL interaction, respectively, was calculated (Fig. 2; Supplemental Material). For the traits plant height, ear weight and total kernel weight, the combination of AMF and AMF x QTL effects explained more than half of the total genetic variation (based on estimation of H^2), and over a quarter of the total phenotypic variance (Fig. 2; Supplemental Material). The identification of significant AMF x QTL effects reveals genetic variation for host response between the CML312 and W22 parents.

The genetic architecture of response variation distinguishes dependence and benefit

As previously described, host response variation confounds differences in dependence and benefit (Fig. 3A; Sawers *et al.*, 2010). Having identified significant AMF x QTL interaction, it was possible to distinguish dependence and benefit by estimating the QTL effect size separately for *AMF-S* and *AMF-R* sub-populations. The effect for QTLs showing significant AMF x QTL differed between *AMF-S* and *AMF-R*. For the majority (12 of 16), the effect was *conditional* - *i.e.* expressed primarily in either *AMF-S* or *AMF-R* families, but not evident in both (Fig. 3B; Des

Marais & Juenger, 2010). Conditional QTLs expressed in *AMF-R* families were considered variation in dependence. Conversely, conditional QTLs expressed in *AMF-S* families were considered variation in benefit (Table 1). By inspection of effect plots (Supplemental material), 8 of the 12 conditional QTLs were classified as dependence QTLs, and the other 4 as benefit QTLs.

Two regions of the genome were associated with multiple QTLs, suggesting a possible shared mechanistic basis: a region on the long arm of chromosome (chr) 1 linked to ear-traits and a region on chr 4 linked to plant height and flowering time (Supplemental material). To combine traits, the complete set was reduced to Principal Components (PCs) and these used in a further QTL analysis (Fig. 4). The first two PCs mapped to these same regions on chr1 and chr4, respectively, consistent with PC trait-loading and the single-trait QTL in these same locations (Supplemental material). The PC1 QTL on chr 1 and the majority of co-localized single-trait QTL were associated with dependence (Fig. 4C; although, see below), plants homozygous for W22 or segregating at the peak marker showing lower values of yield components than CML312 homozygotes in *AMF-R* families; the PC2 QTL on chr 4 and co-localized single trait QTL were associated with benefit, plants carrying the W22 allele conditionally flowering earlier in *AMF-S* families (Fig. 4D).

Antagonistic QTL effects suggest a trade-off between mycorrhizal and non-mycorrhizal growth

Several QTL showed extreme QTL x AMF in which the effect was expressed in both *AMF-S* and *AMF-R* populations, but with a change of sign (*i.e.* a change in the relative performance of the parental alleles) - a condition described as *antagonistic pleiotropy* (Fig. 3C; Table 1.

Supplemental Material; Des Marais & Juenger, 2010). Under such genetic architecture, the superior allele for mycorrhizal plants is detrimental to performance in the absence of mycorrhiza, and *vice versa*, providing evidence for trade-off at the single-locus level. Significantly, several QTLs associated with key yield components showed antagonistic pleiotropy (Fig. 3C; Table 1. These two QTL co-localized with the PC1 QTL on chr 1). Analogous "rank changing" effects can also be seen at the level of the whole genotype (Fig. 5A). Although the mapping design did not permit direct evaluation of the same genotype as both *AMF-S* and *AMF-R*, it was possible to fit QTL models to all genotypes across both levels of AMF. The resulting estimates showed evidence of rank change with respect to performance with or without AMF (Supplemental Material). For example, the genotypes estimated to give the highest values of ear and total kernel weight in mycorrhizal plants were estimated to give the lowest in non-mycorrhizal plants (Fig. 5B). QTL models were built with a small number of QTL for each trait, and their behavior was dominated by the previously mentioned single-locus QTL x AMF effects. To further explore response at the genotype level, whole genome models were used to predict mycorrhizal and non-mycorrhizal trait values across the 137 families. Specifically, *AMF-S* families were used to train a model for mycorrhizal performance that was then applied to all families. Similarly, *AMF-R* families were used to train a model for non-mycorrhizal performance, again subsequently applied to all families. Whole genome predictions aligned well with the observed values of their training sets, although they did not capture the more extreme observed values (Fig. 5C; Supplemental Material). As observed with QTL models, a comparison of mycorrhizal and non-mycorrhizal predictions showed that genotypes associated with the highest values of the major yield components in one condition were unexceptional or poor in the other, indicating a trade-off between benefit and dependence at the whole genotype level (Fig. 5D; Supplemental Material).

Discussion

The importance of AM colonization to maize productivity in a medium-input, rain-fed, subtropical field site was estimated. Extrapolating these observations to a cultivated field planted at 80,000 plants/ha, AM colonization would contribute ~ 2 tonnes/ha to a total yield of ~ 5.5 tonnes/ha, or 38%. Although a rough figure that might be treated with caution, and given that the $F_{2:3}$ families were considerably less productive than commercial hybrids (yields above 10 tonnes/ha are typical in the locality of the trial site), such an estimate still serves to provide a striking indication of the importance of AMF in enhancing maize yield in the field, where the value of AMF has previously been questioned (Ryan and Graham 2018). In a previous evaluation, mutation of a mycorrhiza-specific Pi transporter gene was associated with a 15% reduction in ear-weight (Willmann *et al.*, 2013). Although maize has consistently shown a positive host response when evaluated (e.g. (Kaeppler *et al.*, 2000; Sawers *et al.*, 2017), the impact of AMF in other plant species varies along a continuum from mutualism to parasitism (Johnson *et al.*, 1997; Bergmann *et al.*, 2020). In wild species, host response appears to be centered around neutral commensalistic interactions, with equal occurrence of parasitism and mutualism (Klironomos, 2003). A range of host response is also seen in crop plants (Wen *et al.*, 2019). In sorghum, a close relative of maize, host response varies from positive to negative depending on both the plant variety and the AMF species (Ramírez-Flores *et al.*, unpublished observations; (Watts-Williams *et al.*, 2019). That said, host response has largely been evaluated in young plants, grown under controlled conditions, and such studies may under-estimate the true importance of AM symbiosis in the field over the plant life cycle. In this context, the approach presented here has the potential to be informative in both maize and other species. Although

difficult to speculate on the physiological basis of host response in this trial, the extension of ASI and associated poor seed set in *AMF-R* families is indicative of an overall increase in plant stress. Although well-characterized as a major driver of yield reduction under drought, increasing ASI can also be associated with poor mineral nutrition. Anecdotally, many *AMF-R* families presented chlorosis, indicating nutrient deficiency, but they did not necessarily show symptoms suggesting that P starvation was the primary limitation. In the future, it will be informative to extend the experimental approach through greater physiological evaluation and quantification of plant nutrient levels.

Within the overall host response, there was substantial variation among plant families. Extrapolation of total grain weight at the family level predicts a range of yield response from 0.4 to 3.7 tonnes/ha. In terms of variance explained, AMF x QTL effects were more important than the QTL main effects for total kernel weight, total kernel number and fifty-kernel weight. By considering the conditionality of AMF x QTL effects, it was possible to identify genetic variation in the capacity of the plant to benefit from AM symbiosis, with potential implications for crop improvement. The present analysis is not directly informative as to the mechanisms underlying variation in host response. The level of AM colonization has been reported to differ among varieties in a number of plant species, although greater colonization is not necessarily an indicator of greater host response (Kaeppler *et al.*, 2000; Sawers *et al.*, 2010, 2017; Mascher *et al.*,2014; Watts-Williams *et al.*, 2019; Plouznikoff *et al.*, 2019; Pawlowski *et al.*, 2020). Indeed, the capacity of the host to limit fungal colonization under certain conditions may help to maximize plant benefit, and it is well established that colonization is reduced under nutrient replete conditions (Nouri *et al.*, 2014; Sawers *et al.*, 2017; Karlo *et al.*, 2020). In addition to internal fungal growth, the extent of the root-external hyphal network also significantly impacts

host response (Schweiger & Jakobsen, 1999; Jakobsen *et al.*, 2001; Yao *et al.*, 2001; Munkvold *et al.*, 2004; Schnepf *et al.*, 2008; Sawers *et al.*, 2017). When soil exploration is a greater limitation on nutrient acquisition than the rate of transfer from fungus to plant, the development of root-external hyphae may be more significant than the level of root-internal colonization. Furthermore, certain bacterial taxa exert beneficial and synergistic effects on AM symbiosis (Heijden *et al.*, 2016; Ferreira *et al.*, 2020), acting as so-called "mycorrhiza helper" bacteria (Frey-Klett *et al.*, 2007; Heijden *et al.*, 2016b; Ferreira *et al.*, 2020). Characterization of the root microbiome of *AMF-S* and *AMF-R* families will provide insight into the interplay between AMF, the broader microbial community and host response.

A trade-off was observed between host dependence and benefit: the genotypes predicted to be the best in AM susceptible families were predicted to be unremarkable or poor in the context of AM resistance, and *vice versa*. At the level of individual loci, examples of antagonistic pleiotropy (Des Marais & Juenger, 2010) were seen for QTL associated with days-to-silking, ear weight, total kernel weight, number of kernels per row and fifty kernel weight. Although it is difficult to speculate as to the mechanistic basis of trade-off, the strength of individual QTL effects is promising with respect to future functional analysis. It has been proposed that the differing demands placed on root system architecture and anatomy by direct foraging and AM symbiosis prevent co-optimization for both (Lambers *et al.*, 2008; Wen *et al.*, 2019). For example, although increasing the proportion of root cortical aerenchyma (root air space) reduces the "carbon cost" of the root system, promoting foraging efficiency (Postma & Lynch, 2011), the reduction in cortical tissue may limit AMF colonization and, potentially, host response (Strock *et al.*, 2019). It was somewhat surprising to see a QTL for a morphological trait such as tassel branch number to be conditional on AM susceptibility; such observations may

indicate the action of pleiotropic systemic signals on host plant development. Indeed, the phytohormones well characterized to play diverse roles in plant development (including tassel development) are also implicated in the establishment and regulation of AM symbiosis (Gutjahr, 2014; Sawers *et al.*, 2018; Bonfante & Genre, 2015). For example, disruption of ethylene signalling has been shown to modulate the level of (negative) host response to AMF in *Nicotiana attenuata* (Riedel et al., 2008); a DELLA repressor in the gibberellic acid signalling pathway is essential for AM colonization in rice (Yu *et al.*, 2014); a feedback-loop of CLE peptide-SUNN kinase-strigolactone modulates the extent of AMF colonization in *Medicago truncatula* (Müller *et al.*, 2019). Given that many of these same signals have been the targets of domestication and plant improvement, it is perhaps to be expected that trade-offs will be observed in cultivated plants (Sawers *et al.*, 2018). The QTL x AMF effects underlying trade-offs associated with yield components were primarily driven by plasticity associated with the temperate W22 allele. It is interesting that the CML312 allele, originating from the parent better adapted to the trial conditions, was more stable with respect to susceptibility or resistance to AMF. Our results indicate a potential impact of the interaction between plant genotype and AM community on yield stability.

Supplementary Material

Acknowledgements

We thank Beda Angehrn and Mario Rivera (UNISEM) for assistance with field evaluation, Cruz Robledo (PV Winter Nurseries) for support with generating material, and Jessica Carcaño-Macias for technical support and seed stock management. We acknowledge Karina Picazarri-

Delgado for assistance with preliminary characterization of the *hun* mutants.

Funding

This study was funded by the Mexican National Commission for the Study and Use of Biodiversity (CONABIO) project *Impact of native arbuscular mycorrhizal fungi on maize performance* (Nº 62, 2016-2018). M. Rosario Ramírez-Flores was supported by a Ph.D. scholarship from the Mexican National Council of Science and Technology (CONACYT).

References

Bergmann J, Weigelt A, van der Plas F, Laughlin DC, Kuyper TW, Guerrero-Ramirez N, Valverde-Barrantes OJ, Bruelheide H, Freschet GT, Iversen CM, *et al.* 2020. The fungal collaboration gradient dominates the root economics space in plants. *Science Advances* **6**: eaba3756.

Bonfante P, Genre A. **2015**. Arbuscular mycorrhizal dialogues: do you speak 'plantish' or 'fungish'? *Trends in Plant Science* **20**: 150–154.

Bradbury PJ, Zhang Z, Kroon DE, Casstevens TM, Ramdoss Y, Buckler ES. **2007**. TASSEL: software for association mapping of complex traits in diverse samples. *Bioinformatics* **23**: 2633–2635.

Broman KW, Sen S. **2009**. *A Guide to QTL Mapping with R/qtl*. Springer Science & Business Media.

Broman KW, Wu H, Sen S, Churchill GA. **2003**. R/qtl: QTL mapping in experimental crosses. *Bioinformatics* **19**: 889–890.

Charpentier M, Bredemeier R, Wanner G, Takeda N, Schleiff E, Parniske M. **2008**. Lotus japonicus CASTOR and POLLUX are ion channels essential for perinuclear calcium spiking in legume root endosymbiosis. *The Plant cell* **20**: 3467–3479.

Chiu CH, Paszkowski U. **2019**. Mechanisms and Impact of Symbiotic Phosphate Acquisition. *Cold Spring Harbor perspectives in biology* **11**.

Des Marais DL, Juenger TE. **2010**. Pleiotropy, plasticity, and the evolution of plant abiotic stress tolerance. *Annals of the New York Academy of Sciences* **1206**: 56–79.

Faye A, Dalpé Y, Ndung'u-Magiroi K, Jefwa J, Ndoye I, Diouf M, Lesueur D. **2013**.

Evaluation of commercial arbuscular mycorrhizal inoculants. *Canadian journal of plant science. Revue canadienne de phytotechnie* **93**: 1201–1208.

Ferreira DA, da Silva TF, Pylro VS, Salles JF, Andreote FD, Dini-Andreote F. **2020**. Soil Microbial Diversity Affects the Plant-Root Colonization by Arbuscular Mycorrhizal Fungi. *Microbial ecology*.

Fester T, Sawers R. **2011**. Progress and Challenges in Agricultural Applications of Arbuscular Mycorrhizal Fungi. *Critical Reviews in Plant Sciences* **30**: 459–470.

Frey-Klett P, Garbaye J, Tarkka M. **2007**. The mycorrhiza helper bacteria revisited. *The New phytologist* **176**: 22–36.

Fulton TM, Chunwongse J, Tanksley SD. **1995**. Microprep protocol for extraction of DNA from tomato and other herbaceous plants. *Plant Molecular Biology Reporter* **13**: 207–209.

Gutjahr C. **2014**. Phytohormone signaling in arbuscular mycorhiza development. *Current opinion in plant biology* **20**: 26–34.

Gutjahr C, Banba M, Croset V, An K, Miyao A, An G, Hirochika H, Imaizumi-Anraku H, Paszkowski U. **2008**. Arbuscular mycorrhiza-specific signaling in rice transcends the common symbiosis signaling pathway. *The Plant cell* **20**: 2989–3005.

Heijden MGA van der, van der Heijden MGA, de Bruin S, Luckerhoff L, van Logtestijn RSP, Schlaeppi K. **2016**. A widespread plant-fungal-bacterial symbiosis promotes plant biodiversity, plant nutrition and seedling recruitment. *The ISME Journal* **10**: 389–399.

Hetrick BAD, Wilson GWT, Cox TS. **1992**. Mycorrhizal dependence of modern wheat varieties, landraces, and ancestors. *Canadian Journal of Botany* **70**: 2032–2040.

Jakobsen I, Gazey C, Abbott LK. **2001**. Phosphate transport by communities of arbuscular mycorrhizal fungi in intact soil cores. *New Phytologist* **149**: 95–103.

Janos DP. **2007**. Plant responsiveness to mycorrhizas differs from dependence upon mycorrhizas. *Mycorrhiza* **17**: 75–91.

Johnson NC, Graham JH, Smith FA. **1997**. Functioning of mycorrhizal associations along the mutualism-parasitism continuum. *New Phytologist* **135**: 575–585.

Kaeppler SM, Parke JL, Mueller SM, Senior L, Stuber C, Tracy WF. **2000**. Variation among Maize Inbred Lines and Detection of Quantitative Trait Loci for Growth at Low Phosphorus and Responsiveness to Arbuscular Mycorrhizal Fungi. *Crop science* **40**: 358.

Karlo M, Boschiero C, Landerslev KG, Blanco GS, Wen J, Mysore KS, Dai X, Zhao PX, de Bang TC. **2020**. The CLE53-SUNN genetic pathway negatively regulates arbuscular mycorrhiza root colonization in Medicago truncatula. *Journal of experimental botany*.

Klironomos JN. **2003**. VARIATION IN PLANT RESPONSE TO NATIVE AND EXOTIC

ARBUSCULAR MYCORRHIZAL FUNGI. *Ecology* **84**: 2292–2301.

Lambers H, Raven JA, Shaver GR, Smith SE. **2008**. Plant nutrient-acquisition strategies change with soil age. *Trends in ecology & evolution* **23**: 95–103.

Lynch JP. **2019**. Root phenotypes for improved nutrient capture: an underexploited opportunity for global agriculture. *The New phytologist* **223**: 548–564.

Mascher M, Gerlach N, Gahrtz M, Bucher M, Scholz U, Dresselhaus T. **2014**. Sequence and ionomic analysis of divergent strains of maize inbred line B73 with an altered growth phenotype. *PloS one* **9**: e96782.

McCarty DR, Settles AM, Suzuki M, Tan BC, Latshaw S, Porch T, Robin K, Baier J, Avigne W, Lai J, *et al.* 2005. Steady-state transposon mutagenesis in inbred maize. *The Plant journal: for cell and molecular biology* **44**: 52–61.

Merchant N, Lyons E, Goff S, Vaughn M, Ware D, Micklos D, Antin P. **2016**. The iPlant Collaborative: Cyberinfrastructure for Enabling Data to Discovery for the Life Sciences. *PLoS biology* **14**: e1002342.

Miller ND, Haase NJ, Lee J, Kaeppler SM, de Leon N, Spalding EP. **2017**. A robust, high-throughput method for computing maize ear, cob, and kernel attributes automatically from images. *The Plant journal: for cell and molecular biology* **89**: 169–178.

Müller LM, Flokova K, Schnabel E, Sun X, Fei Z, Frugoli J, Bouwmeester HJ, Harrison MJ. **2019**. A CLE-SUNN module regulates strigolactone content and fungal colonization in arbuscular mycorrhiza. *Nature plants* **5**: 933–939.

Munkvold L, Kjøller R, Vestberg M, Rosendahl S, Jakobsen I. **2004**. High functional diversity within species of arbuscular mycorrhizal fungi. *New Phytologist* **164**: 357–364.

Nouri E, Breuillin-Sessoms F, Feller U, Reinhardt D. **2014**. Phosphorus and nitrogen regulate arbuscular mycorrhizal symbiosis in Petunia hybrida. *PloS one* **9**: e90841.

Parniske M. **2008**. Arbuscular mycorrhiza: the mother of plant root endosymbioses. *Nature reviews. Microbiology* **6**: 763–775.

Pawlowski ML, Vuong TD, Valliyodan B, Nguyen HT, Hartman GL. **2020**. Whole-genome resequencing identifies quantitative trait loci associated with mycorrhizal colonization of soybean. *TAG. Theoretical and applied genetics. Theoretische und angewandte Genetik* **133**: 409–417.

Plouznikoff K, Asins MJ, de Boulois HD, Carbonell EA, Declerck S. **2019**. Genetic analysis of tomato root colonization by arbuscular mycorrhizal fungi. *Annals of botany* **124**: 933–946.

Postma JA, Lynch JP. **2011**. Root cortical aerenchyma enhances the growth of maize on soils with suboptimal availability of nitrogen, phosphorus, and potassium. *Plant physiology* **156**: 1190–1201.

Ramírez-Flores MR. 2015. Caracterización genética de mutantes de HUN e IXBA, ortólogos de maíz de los canales de potasio CASTOR y POLLUX. M.Sc. thesis. Centro de Investigación y de Estudios Avanzados del Instituto Politécnico Nacional. Guanajuato, Mexico.

Riedel T, Groten K, Baldwin IT. **2008**. Symbiosis between Nicotiana attenuata and Glomus intraradices: ethylene plays a role, jasmonic acid does not. *Plant, cell & environment* **31**: 1203–1213.

Sawers RJH, Gebreselassie MN, Janos DP, Paszkowski U. **2010**. Characterizing variation in mycorrhiza effect among diverse plant varieties. *TAG. Theoretical and applied genetics. Theoretische und angewandte Genetik* **120**: 1029–1039.

Sawers RJH, Gutjahr C, Paszkowski U. **2008**. Cereal mycorrhiza: an ancient symbiosis in modern agriculture. *Trends in plant science* **13**: 93–97.

Sawers RJH, Ramírez-Flores MR, Olalde-Portugal V, Paszkowski U. **2018**. The impact of domestication and crop improvement on arbuscular mycorrhizal symbiosis in cereals: insights from genetics and genomics. *The New phytologist* **220**: 1135–1140.

Sawers RJH, Svane SF, Quan C, Grønlund M, Wozniak B, Gebreselassie M-N, González-Muñoz E, Chávez Montes RA, Baxter I, Goudet J, *et al.* 2017. Phosphorus acquisition efficiency in arbuscular mycorrhizal maize is correlated with the abundance of root-external hyphae and the accumulation of transcripts encoding PHT1 phosphate transporters. *The New phytologist* **214**: 632–643.

Schnepf A, Roose T, Schweiger P. **2008**. Impact of growth and uptake patterns of arbuscular mycorrhizal fungi on plant phosphorus uptake—a modelling study. *Plant and Soil* **312**: 85–99.

Schweiger PF, Jakobsen I. **1999**. Direct Measurement of Arbuscular Mycorrhizal Phosphorus Uptake into Field-Grown Winter Wheat. *Agronomy Journal* **91**: 998–1002.

Strock CF, Schneider HM, Galindo-Castañeda T, Hall BT, Van Gansbeke B, Mather DE, Roth MG, Chilvers MI, Guo X, Brown K, *et al.* 2019. Laser ablation tomography for visualization of root colonization by edaphic organisms. *Journal of experimental botany* **70**: 5327–5342.

Strullu-Derrien C, Selosse M-A, Kenrick P, Martin FM. **2018**. The origin and evolution of mycorrhizal symbioses: from palaeomycology to phylogenomics. *The New phytologist* **220**: 1012–1030.

Taylor J, Butler D. **2017**. R Package ASMap: Efficient Genetic Linkage Map Construction and Diagnosis. *Journal of Statistical Software* **79**.

Watts-Williams SJ, Emmett BD, Levesque-Tremblay V, MacLean AM, Sun X, Satterlee JW, Fei Z, Harrison MJ. **2019a**. Diverse Sorghum bicolor accessions show marked variation in growth and transcriptional responses to arbuscular mycorrhizal fungi. *Plant, cell & environment* **42**: 1758–1774.

Watts-Williams SJ, Emmett BD, Levesque-Tremblay V, MacLean AM, Sun X, Satterlee JW, Fei Z, Harrison MJ. **2019b**. Diverse Sorghum bicolor accessions show marked variation in growth and transcriptional responses to arbuscular mycorrhizal fungi. *Plant, cell & environment* **42**: 1758–1774.

Wen Z, Li H, Shen Q, Tang X, Xiong C, Li H, Pang J, Ryan MH, Lambers H, Shen J. **2019**. Tradeoffs among root morphology, exudation and mycorrhizal symbioses for phosphorus-acquisition strategies of 16 crop species. *The New phytologist* **223**: 882–895.

Willmann M, Gerlach N, Buer B, Polatajko A, Nagy R, Koebke E, Jansa J, Flisch R, Bucher M. **2013**. Mycorrhizal phosphate uptake pathway in maize: vital for growth and cob development on nutrient poor agricultural and greenhouse soils. *Frontiers in plant science* **4**: 533.

Yao Q, Li X, Feng G, Christie P. **2001**. Influence of extramatrical hyphae on mycorrhizal dependency of wheat genotypes. *Communications in Soil Science and Plant Analysis* **32**: 3307–3317.

Yu N, Luo D, Zhang X, Liu J, Wang W, Jin Y, Dong W, Liu J, Liu H, Yang W, *et al.* 2014. A DELLA protein complex controls the arbuscular mycorrhizal symbiosis in plants. *Cell research* **24**: 130–133.

565 **Table 1. Summary of host response and QTLs**

Trait	Mean AMF-S	Mean AMF-R	Adj. P-value[1]	HR[2]	HR (%)[3]	QTLs[4]	AMFxQTL[5]	Type[6]
STD	11	10	NS	1	10			
DTA	56	57	NS	-1	-1	1	1	S
DTS	59	60	***	-1	-3	1	1	AP
ASI	2	4	***	-2	-34	1	1	R
PH	196.8	171.8	***	25	15	2	2	R, S
TBN	13	12	NS	1	10	2	1	C, S
GC				0		1	0	C
EW	86.6	60.6	***	26	43	2	2	AP, S
EL	13.9	12.4	***	1.5	13	1	1	R
ED	40.3	37.2	***	3.1	8	2	2	R, R
KRN	16	15	*	1	6	1	0	C
KPR	25	18	***	7	37	2	2	R, AP
KC				0		1	0	C
CD	26.6	26.1	NS	0.5	2			
FKW	10.4	9.4	NS	1	10	2	2	R, AP
TKW	67.7	44.8	***	22.9	51	1	1	AP
TKN	330	230	***	100	44	1	1	R

[1]Wilcoxon tests with Bonferonni adjusted P-values. Note: *: $p < 0.05$; **: $p < 0.01$; ***: $p < 0.001$; NS: not significant. [2]Host response calculated as mean *AMF-S* - *AMF-R*. [3]Host response expressed as percentage of *AMF-R* mean. [4]Number of QTL associated with a given trait. [5]Number of QTL showing significant QTL x AMF effect. [6]Pattern of QTL x AMF effect: R: conditional on *AMF-R*; S, conditional on *AMF-S*; AP, antagonistic pleiotropy; C, constitutive. Trait codes: STD, stand count; DTA, days to anthesis; DTS, days to silking; ASI, anthesis-silking interval; PH, plant height; TBN, tassel branch number; EW, ear weight; EL, ear length; ED, ear diameter; KRN, kernel row number; KPR, kernels per row; CD, cob diameter; FKW, fifty kernel weight; TKW, total kernel weight; TKN, total kernel number.

Figure Legends

Figure 1. Mycorrhizal symbiosis impacts maize growth under cultivation. A, Susceptible (*AMF-S*) and resistant (*AMF-R*) families segregate genomic content from two founder parents, shown as red and blue bars. *AMF-R* families are homozygous for the *hun1-2* mutation, blocking AM symbiosis (black arrows). **B**, Border between representative *AMF-S* and *AMF-R* plots, Jalisco, Mexico, 2019. **C**, Representative AMF-S ears. **D**, Representative AMF-R ears. **E**, Plant height (PH) of 73 *AMF-S* and 64 *AMF-R* families. **F**, Kernel shape (KS). **G**, Anthesis-silking interval (ASI). **H**, Total kernel number (TKN). The violin plots in **E, F** and **H** are a hybrid of boxplot and density plot. The box represents the interquartile range with the horizontal line representing the median and whiskers representing 1.5 times the interquartile ranges. The shape of the violin plot represents probability density of data at different values along the y-axis.

Figure 2. QTL x AMF effects contribute significantly to variation in MR. The contribution to phenotypic variance in different plant traits among 137 *AMF-S*/*AMF-R* families. Total genetic variance (H^2) was estimated based on differences between experimental blocks. Variance explained by the QTL model for each trait is partitioned into that explained by the additive effect of AMF, the additional variation explained by interactive QTL and QTL x AMF interaction (QTL x AMF) and the additional variation explained by non-additive QTL. Traits codes as in Table 1.

Figure 3. Mycorrhiza response confounds benefit and dependence. A, host response (R) is the difference in trait value between mycorrhizal (M; green) and non-mycorrhizal (NM, yellow) plants. Increased response can result from either greater dependence (D; poorer performance of

NM plants) or greater benefit (B; greater performance of M plants). **B**, QTL x AMF effects underlying variation in response reveal the balance of benefit and dependence. The difference in trait value between plants carrying the CML312 (red) or W22 (blue) allele. In this theoretical example, the effect is conditional on mycorrhizal colonization, reflecting a difference in benefit more than dependence. **C**, QTL effects for a total kernel weight (TKW) QTL located on Chromosome 1. TKW of families homozygous for the CML312 allele at this locus (red) is stable across susceptible (*AMF-S*) and resistant (*AMF-R*) families. In contrast, families homozygous for the W22 allele (blue) or segregating at this locus (brown), show superior TKW if *AMF-S* but lower TKW if *AMF-R*. In this extreme example of QTL x AMF, the QTL is linked to differences in both dependence and benefit, an example of antagonistic pleiotropy or "trade-off".

Figure 4. Trait PCs capture variation in both dependence and benefit. A, Phenotypic variation captured by the first five principal components (PCs). **B**, Loading of *AMF-S* and *AMF-R* families on PC1 and PC2. The position of trait names (as Table 1) with respect to the origin indicates contribution to each PC. **C, D,** effect plots for major QTL associated with PC1 and PC2, respectively. The PC1 QTL is conditional on *AMF-R*, indicating a difference in dependence. The PC2 QTL is conditional on *AMF-S*, indicating a difference in benefit.

Figure 5. The genetic architecture of mycorrhiza response implies a trade-off between dependence and benefit. A, Theoretical trade-off between the performance of non-mycorrhizal (NM) and mycorrhizal (M) plants. For any position on this plot, the vertical distance above the diagonal indicates the magnitude of host response. Trade-off prevents occupancy of the upper-right of the plot, defining a so-called "Pareto front" (solid arc). Here, an increase in the NM

performance of variety X is necessarily accompanied by a reduction in M performance, as described by movement along the arc to condition Y. Biological constraint prevents the path towards condition Z which would represent NM improvement without any negative impact on M. **B**, Fitted ear weight values for all genotypes from the QTL model (2 QTL and their interactions with AMF) under both levels of AMF (*AMF-S* and *AMF-R*). Line segments connect the same QTL genotype under the two AMF levels. **C**, Observed ear weight against whole-genome prediction for 73 susceptible (*AMF-S*) and 64 resistant (*AMF-R*) families. **D**, Predicted ear weights for all 137 genotypes based on *AMF-S* (M) and *AMF-R* (NC) whole-genome models. Point colour indicates the AMF susceptibility of the original family.

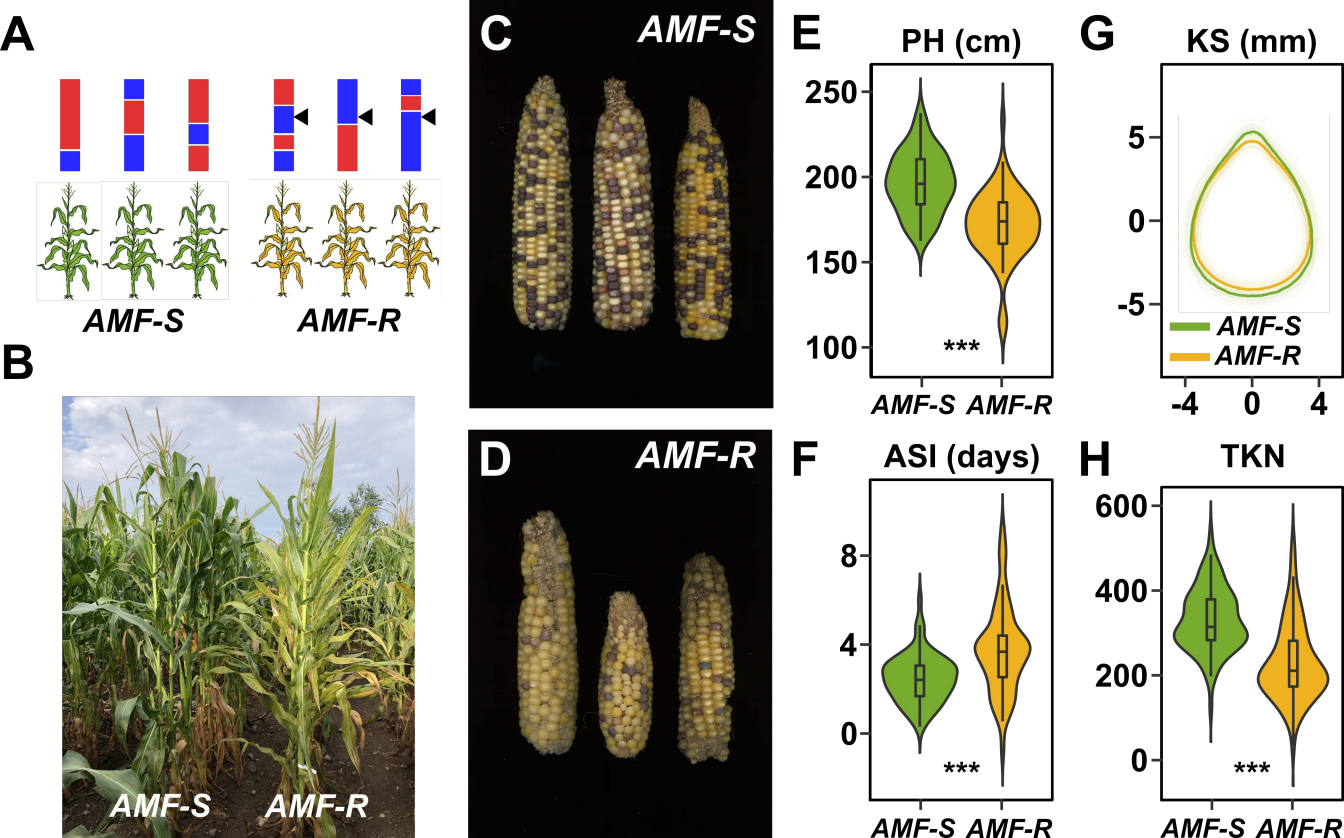
A
AMF-S
AMF-R
B
AMF-S
AMF-R
C
AMF-S
D
AMF-R
E
PH (cm)
250
200
150
100
***
AMF-S
AMF-R
F
ASI (days)
8
4
0
***
AMF-S
AMF-R
G
KS (mm)
5
0
-5
-4
0
4
AMF-S
AMF-R
H
TKN
600
400
200
0
***
AMF-S
AMF-R

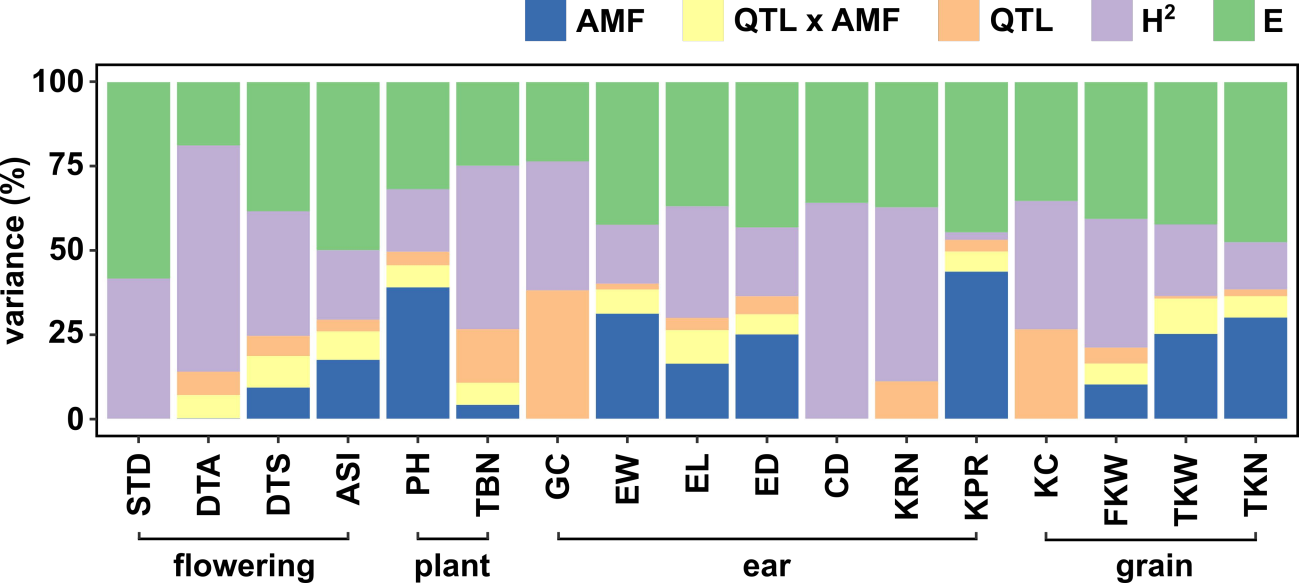
AMF
QTL x AMF
QTL
H2
E
variance (%)
100
75
50
25
0
STD
DTA
DTS
ASI
PH
TBN
GC
EW
EL
ED
CD
KRN
KPR
KC
FKW
TKW
TKN
flowering
plant
ear
grain

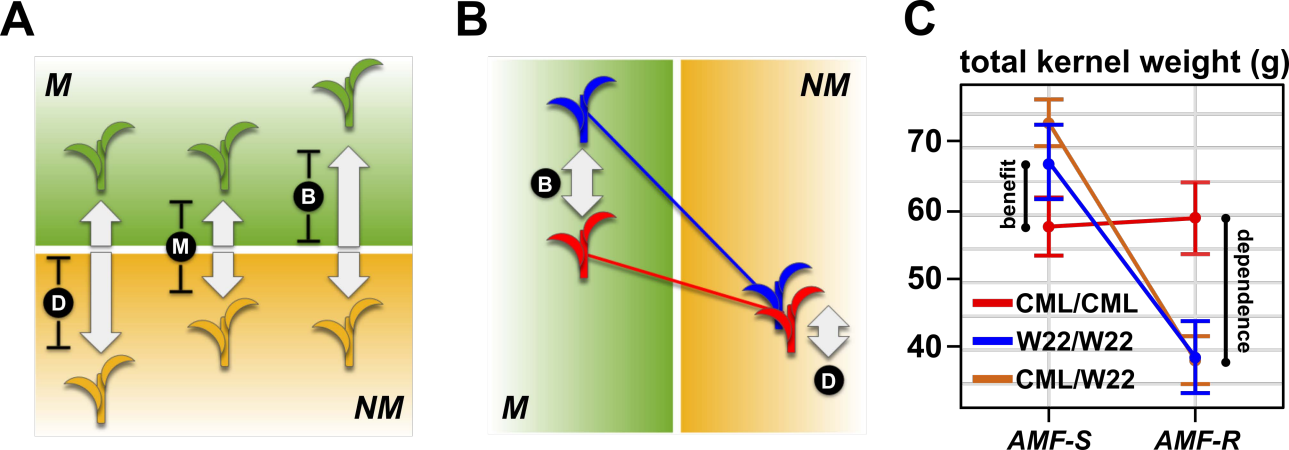
A
M
NM
B
M
D
B
NM
M
D
C
total kernel weight (g)
70
60
50
40
benefit
dependence
CML/CML
W22/W22
CML/W22
AMF-S
AMF-R

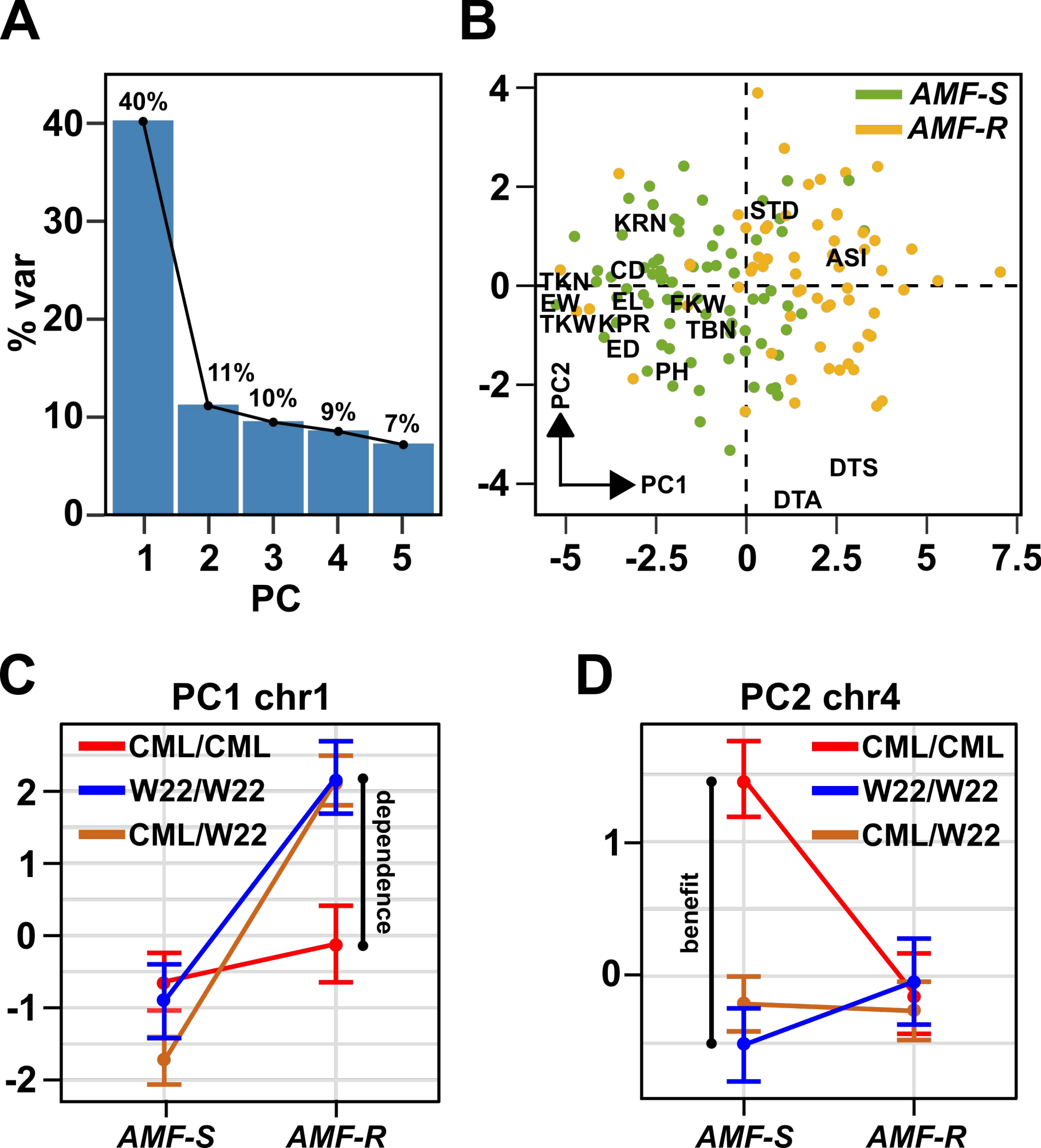
A
40%
11%
10%
9%
7%
% var
PC
B
AMF-S
AMF-R
KRN
STD
ASI
CD
TKN
EW
EL
FKW
TKW
KPR
TBN
ED
PH
DTS
DTA
PC2
PC1
C
PC1 chr1
CML/CML
W22/W22
CML/W22
dependence
AMF-S
AMF-R
D
PC2 chr4
CML/CML
W22/W22
CML/W22
benefit
AMF-S
AMF-R

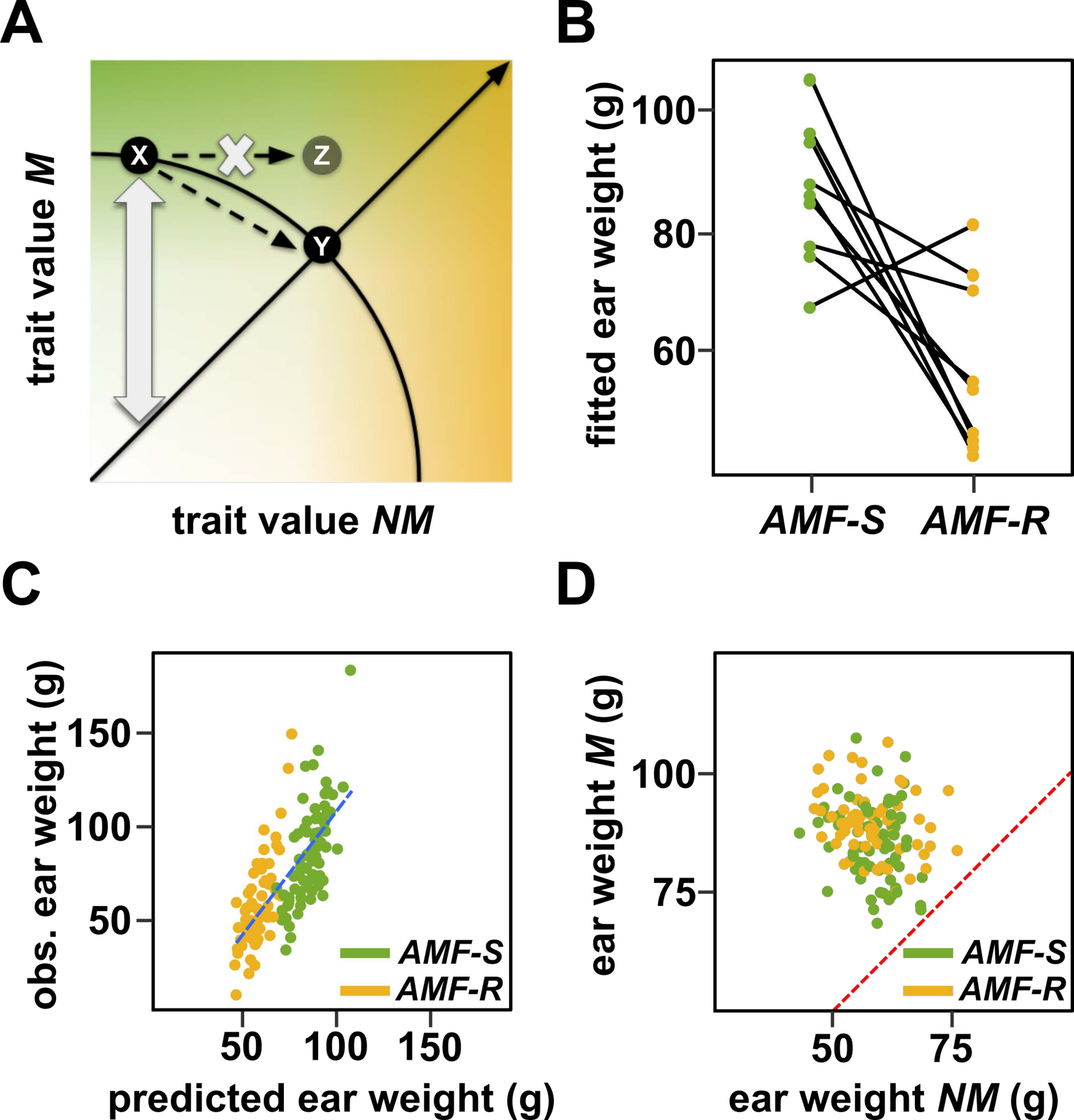
A
X
Z
Y
trait value M
trait value NM
B
fitted ear weight (g)
100
80
60
AMF-S
AMF-R
C
obs. ear weight (g)
150
100
50
AMF-S
AMF-R
50
100
150
predicted ear weight (g)
D
ear weight M (g)
100
75
AMF-S
AMF-R
50
75
ear weight NM (g)